

# Effect of B<sub>2</sub>O<sub>3</sub> content on crack initiation under Vickers indentation test

Yoshinari KATO,<sup>\*,\*\*,†</sup> Hiroki YAMAZAKI,<sup>\*</sup> Yoshihiro KUBO,<sup>\*\*</sup> Satoshi YOSHIDA,<sup>\*\*</sup>  
Jun MATSUOKA<sup>\*\*</sup> and Tomoko AKAI<sup>\*\*\*</sup>

<sup>\*</sup>Technical Division, Nippon Electric Glass Co., Ltd., Otsu, Shiga 520-8639

<sup>\*\*</sup>School of Engineering, The University of Shiga Prefecture, Hikone, Shiga 522-8533

<sup>\*\*\*</sup>Research institute for Innovation in Sustainable Chemistry, National Institute of Advanced Industrial Science and Technology (AIST), Ikeda, Osaka 562-8577

Effect of B<sub>2</sub>O<sub>3</sub> content on crack resistance was investigated by indentation tests of glass samples with various compositions of B<sub>2</sub>O<sub>3</sub>. The ternary SiO<sub>2</sub>-B<sub>2</sub>O<sub>3</sub>-Na<sub>2</sub>O glass system (SBN series) and non-alkaline aluminoborosilicate glass system (SAB series). When B<sub>2</sub>O<sub>3</sub> is substituted with SiO<sub>2</sub> in the SBN system ("SBN1" series), crack resistance has a relationship with density. In a series of the SBN system where density did not change with B<sub>2</sub>O<sub>3</sub> content ("SBN2" series), crack resistance decreased with increasing B<sub>2</sub>O<sub>3</sub> content. On the other hand, crack resistance increased with increasing B<sub>2</sub>O<sub>3</sub> content in the SAB series, where density did not change. According to the results of NMR measurement, boron in 4-coordination state (<sup>4</sup>B) increased in the SBN2 series while boron in 3-coordination state (<sup>3</sup>B) increased in the SAB series with increasing B<sub>2</sub>O<sub>3</sub> content. Therefore, crack resistance increases with increasing <sup>3</sup>B and decreases with increasing <sup>4</sup>B. The difference in structure between <sup>3</sup>B and <sup>4</sup>B containing glasses leads to different effect on residual stress around the indentation, resulting in difference in crack resistance.

©2010 The Ceramic Society of Japan. All rights reserved.

Key-words : Oxide glass, Crack initiation, Indentation, B<sub>2</sub>O<sub>3</sub>

[Received March 25, 2010; Accepted June 17, 2010]

## 1. Introduction

Crack initiation and crack propagation are the most important factors determining strength of glass. It is well known that glass shows very high theoretical strength close to 10 GPa. However, once a crack initiates in the glass surface, stress concentration occurs at the crack tip, resulting in catastrophic fracture by applied stress much lower than the theoretical strength. So evaluation of crack initiation and crack propagation is of much interest for glass engineers and glass scientists.

Crack propagation is usually evaluated by measuring fracture toughness,  $K_{IC}$ . It is expected that glass with higher  $K_{IC}$  has higher breaking strength. Although various glass compositions show almost the same value of  $K_{IC}$ , there is much difference in susceptibility of fracture in industrial and practical use among glass compositions. It is supposed that the difference is due to a difference of crack initiation. Therefore, both characteristics of crack initiation and crack propagation must be evaluated for understanding glass strength.

Some methods for evaluating crack initiation of glass were proposed. Wada et al.<sup>1)</sup> proposed "crack resistance ( $CR$ )" of glass against Vickers indentation. When a glass sample is indented with a Vickers diamond indenter, radial cracks initiate around the indentation at a given indentation load. The value of  $CR$  is defined as the load for the radial cracks to initiate, indicating the difficulty in crack initiation. On the other hand, Lawn et al.<sup>2)</sup> proposed the ratio of hardness to fracture toughness as a simple index of brittleness, and Sehgal et al.<sup>3)</sup> developed a convenient method to estimate the "brittleness" index of glass by using the ratio of characteristic crack length to the length of indentation diagonal.

In our previous study,<sup>4)</sup>  $CR$  of various commercial glass compositions are investigated by using Vickers indentations, and compared with other mechanical properties. The value of  $CR$  does not have a clear relationship with  $K_{IC}$ , but it has a clear relationship with recovery of indentation depth ( $RID$ ). The value of  $RID$  is calculated by using a difference between indentation depth before and after heat-treatment, and it shows degree of densification. The value increased with increasing  $RID$ . It is concluded that densification should reduce residual stress around the indentation to prevent cracks from initiating.

As mentioned above, a clear relationship between  $CR$  and conventional mechanical properties has not been found, but it was found that there is difference in  $CR$  between glass with more B<sub>2</sub>O<sub>3</sub> content and glass with less B<sub>2</sub>O<sub>3</sub> content. The relationship between  $CR$  and  $K_{IC}$  is shown in Fig. 1. There is a trend that  $CR$  increases with increasing  $K_{IC}$  among the glass containing less than 5% B<sub>2</sub>O<sub>3</sub>. On the other hand, glasses containing more B<sub>2</sub>O<sub>3</sub> show higher  $CR$  compared with this trend. Therefore, it is supposed that B<sub>2</sub>O<sub>3</sub> content may increase  $CR$ . However, there is no report on the effect of B<sub>2</sub>O<sub>3</sub> content on  $CR$ . In the present study,  $CR$  of glass in the ternary system SiO<sub>2</sub>-B<sub>2</sub>O<sub>3</sub>-Na<sub>2</sub>O system ("SBN" series) and in non-alkaline aluminoborosilicate glass system ("SAB" series) is evaluated, and effect of B<sub>2</sub>O<sub>3</sub> content on  $CR$  is discussed.

## 2. Experimental

### 2.1 Preparation of glass sample

Three glass compositional series were selected in this study. Two of them are simple ternary series of SiO<sub>2</sub>-B<sub>2</sub>O<sub>3</sub>-Na<sub>2</sub>O (SBN series). The compositions in the SBN series employed in this study are shown in Fig. 2. The "SBN1" series is expressed by (80 - 40x)SiO<sub>2</sub>-40xB<sub>2</sub>O<sub>3</sub>-20Na<sub>2</sub>O ( $x = 0, 0.125, 0.25, 0.5, 0.75,$  and 1.0) and the "SBN2" series is expressed by 80SiO<sub>2</sub>-

<sup>†</sup> Corresponding author: Y. Kato; E-mail: ykato@neg.co.jp

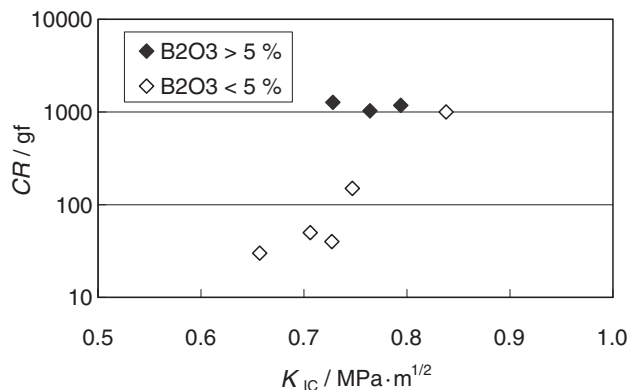


Fig. 1. A relationship between fracture toughness  $K_{IC}$  and crack resistance  $CR$ . This figure is reproduced after Kato et al.<sup>4)</sup>

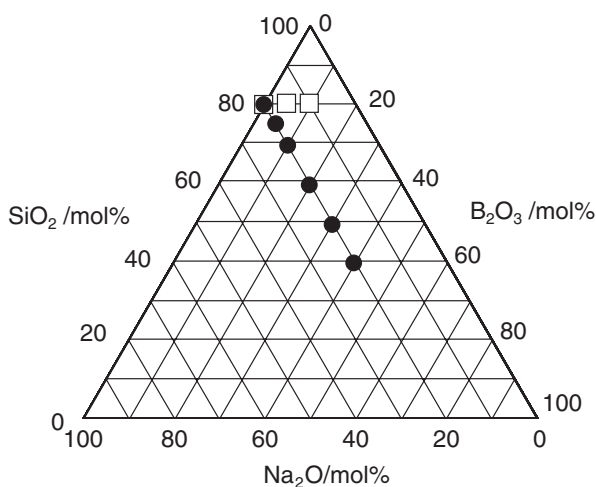


Fig. 2. Batch compositions of samples studied in the SBN series. Solid circles denote glass composition in the  $(80 - 40x)\text{SiO}_2 - 40xB_2\text{O}_3 - 20\text{Na}_2\text{O}$  series, “SBN1” ( $x = 0, 0.125, 0.25, 0.5, 0.75, \text{ and } 1.0$ ). Open squares denote glass composition in the  $80\text{SiO}_2 - 10y\text{B}_2\text{O}_3 - (20 - 10y)\text{Na}_2\text{O}$  series, “SBN2” ( $y = 0, 0.5, \text{ and } 1.0$ ).

$10y\text{B}_2\text{O}_3 - (20 - 10y)\text{Na}_2\text{O}$  ( $y = 0, 0.5, \text{ and } 1.0$ ). Phase separation was not observed with microscope in all of the samples prepared in this study. The other system is non-alkaline aluminoborosilicate system, “SAB series”. The glass compositions in this SAB series correspond to those obtained by substituting  $\text{SiO}_2$  with  $\text{B}_2\text{O}_3$  by 2.5 mol% or 5.0 mol% in composition of a commercial non-alkaline aluminoborosilicate glass. The general composition of the commercial glass is as follows:  $70\text{SiO}_2, 10\text{Al}_2\text{O}_3, 10\text{B}_2\text{O}_3, 6\text{CaO}, 3\text{SrO}, 1\text{BaO}$  (by mol%), and other minor components. Therefore, the glass composition in the SAB series investigated in this study is expressed approximately by the equation of  $(70 - z)\text{SiO}_2 - 10\text{Al}_2\text{O}_3 - (10 + z)\text{B}_2\text{O}_3 - 6\text{CaO} - 3\text{SrO} - 1\text{BaO}$  ( $z = 0.0, 2.5, \text{ and } 5.0$ ). Each glass composition is rewritten in molar percentage in **Table 1**.

Glass samples were prepared by melting the batch of high-grade raw materials which are used for manufacturing glass for electrical use. For the SBN system, the powders of the raw material  $\text{SiO}_2, \text{B}_2\text{O}_3, \text{ and } \text{Na}_2\text{CO}_3$  were weighed appropriately, and a little of refining agent corresponding to a few tenth percentage was added to prepare batches. The batches were mixed thoroughly and melted in a 500 cc Pt crucibles at 1100 to 1500°C for about 6 h in an electric furnace. The melting temperature for each composition was chosen according to the

**Table 1.** Batch compositions of the samples in the SBN series and the SAB series. The SBN1 series and the SBN2 series are expressed by the equations of  $(80 - 40x)\text{SiO}_2 - 40xB_2\text{O}_3 - 20\text{Na}_2\text{O}$  and  $80\text{SiO}_2 - 10y\text{B}_2\text{O}_3 - (20 - 10y)\text{Na}_2\text{O}$ , respectively. The SAB series is expressed approximately by the equation  $(70 - z)\text{SiO}_2 - 10\text{Al}_2\text{O}_3 - (10 + z)\text{B}_2\text{O}_3 - 6\text{CaO} - 3\text{SrO} - 1\text{BaO}$

	$\text{SiO}_2$ (mol %)	$\text{B}_2\text{O}_3$ (mol %)	$\text{Na}_2\text{O}$ (mol %)	$\text{Al}_2\text{O}_3$ (mol %)	$\text{CaO}$ (mol %)	$\text{SrO}$ (mol %)	$\text{BaO}$ (mol %)
SBN1 series							
$x = 0.0$	80	0	20	—	—	—	—
$x = 0.125$	75	5	20	—	—	—	—
$x = 0.25$	70	10	20	—	—	—	—
$x = 0.5$	60	20	20	—	—	—	—
$x = 0.75$	50	30	20	—	—	—	—
$x = 1.0$	40	40	20	—	—	—	—
SBN2 series							
$y = 0.0$	80	0	20	—	—	—	—
$y = 0.5$	80	5	15	—	—	—	—
$y = 1.0$	80	10	10	—	—	—	—
SAB system							
$z = 0.0$	70	10	—	10	6	3	1
$z = 2.5$	67.5	12.5	—	10	6	3	1
$z = 5.0$	65	15	—	10	6	3	1

viscosity of the melt. For the SAB series, the raw material  $\text{SiO}_2, \text{Al}_2\text{O}_3, \text{B}_2\text{O}_3, \text{CaCO}_3, \text{SrCO}_3, \text{BaCO}_3,$  and other minor components were used. The powders were melted at 1500°C for about 22 h. After the melting mentioned above, the glass melts were poured onto a carbon plate, and then placed in an electric furnace to cool slowly. Glass transition temperature,  $T_g$ , was determined by a dilatometer. The cooled glass was heated up to the temperature of  $(T_g + 30^\circ\text{C})$ , held for 30 min, and then cooled by  $3^\circ\text{C}/\text{min}$  to obtain annealed glasses. Samples of the glasses were ground, lapped with  $\text{Al}_2\text{O}_3$  slurry, and then finished with cerium oxide to get optically smooth surfaces, which were used for the following indentation tests.

## 2.2 Measurement of glass properties

The properties, that is, density ( $\rho$ ), glass transition temperature ( $T_g$ ), Young’s modulus ( $E$ ), and bulk modulus ( $K$ ), are measured. Density was measured by Archimedes method. Young’s modulus and shear modulus ( $G$ ), were determined by cube-resonance method.<sup>5)</sup> Bulk modulus was calculated by using the values of  $E$  and  $G$ . The Vickers hardness was measured with a microhardness tester (MXT50, Matsuzawa Seiki Corp., Japan). The applied load was 100 gf.

The value of  $CR$  was measured by Vickers indentation tests.<sup>1)</sup> The glass sample was indented by a Vickers diamond indenter in air ( $25^\circ\text{C}, 30\%$  relative humidity), and the corners where radial cracks appeared were counted using an optical microscope. When glass sample is indented, various types of crack initiate around the indenter. Only radial cracks are counted for determining crack resistance, because the cracks normal to glass surface are critical to fracture of glass. The percentage of crack initiation was determined as the ratio of the number of the corners with the cracks to the total number of the corners of indentations. The applied load was increased step-by-step and twenty indentations were made for each applied load. The load at which the percentage would be 50% is determined as “crack resistance” or  $CR$ . The details of the method to measure  $CR$  are described in our previous paper.<sup>4)</sup>

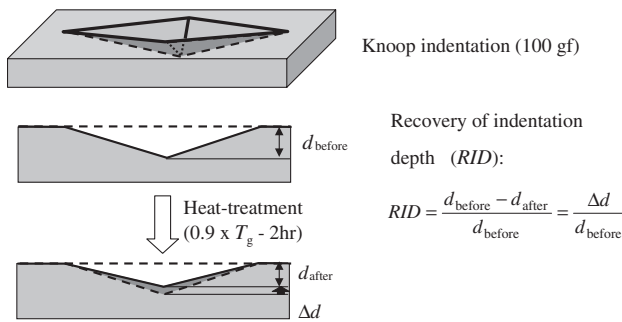


Fig. 3. Schematics of measuring recovery of indentation depth or RID.

Densification was evaluated by shrinkage of indentation through heat-treatment.<sup>6)–9)</sup> The shrinkage is attributed to annealing recovery of densified glass under high compressive stress.<sup>10)</sup> The procedure to measure the recovery of indentation depth is shown in Fig. 3. A glass sample was indented with a Knoop indenter at an applied load of 100 gf, and the depth of the indentation was measured by an atomic force microscope, AFM (Nanoscope IIIa Digital Instrument, USA). A Knoop indenter was used because of its tendency to inhibit crack formation. The indented sample was heat-treated at temperature of  $0.9 \times T_g$  (in °C) for 2 hours, and the indentation depth was measured again. The ratio of the depth change to the depth before the heat-treatment was defined as recovery of indentation depth or RID as the following equation,

$$RID = (d_{\text{before}} - d_{\text{after}}) / d_{\text{before}} = \Delta d / d_{\text{before}}. \quad (1)$$

Here,  $d_{\text{before}}$  and  $d_{\text{after}}$  are Knoop indentation depths before and after the heat-treatment, respectively, and  $\Delta d$  is difference between the depths. The details of the method are also described in our previous paper.<sup>4)</sup>

### 2.3 NMR measurement

By using NMR, coordination state of boron was determined. It is well known that there is two types of coordination state of boron in glass: 3-coordination state (<sup>3</sup>B) and 4-coordination state (<sup>4</sup>B). <sup>11</sup>B NMR spectra were collected with a Chemmag-netics CMX-200 spectrometer (4.7 T) at a resonance frequency of 64.25 MHz. The 90° pulse length is 4.5 μs. All spectra were recorded using 0.5 μs pulse excitation. Delay time of 3 s was used. The fractions of 4-coordinated boron,  $N_4$ , and 3-coordinated boron,  $N_3$ , were obtained by simulating the NMR line shape with a home-built software developed by National Institute of Advanced Industrial Science and Technology (AIST), Japan.<sup>11)</sup>

## 3. Results

Results of  $\rho$ ,  $T_g$ ,  $E$ ,  $K$ , and  $H_v$  are shown in Table 2. In the SBN1 series, density increases with increasing  $x$ , shows a maximum at  $x = 0.5$ , and then decreases. The values of  $T_g$ ,  $E$ ,  $K$ , and  $H_v$  show maxima at  $x = 0.5$ . In the SBN2 series, there is no change in density as a function of  $y$ . The values of  $T_g$ ,  $E$ ,  $K$ , and  $H_v$  increases with increasing  $y$  (increasing B<sub>2</sub>O<sub>3</sub>). In the SAB series, density does not change with increasing  $z$ , similar to the SBN2 series. However, unlike the SBN2 series, the values of  $T_g$ ,  $E$ , and  $K$  decrease with increasing  $z$ .

The relationship between indentation load and percentage of crack initiation in the SBN1, the SBN2, and the SAB series are shown in Figs. 4(a), (b), and (c), respectively. The percentage of crack initiation increases with increasing the applied load. From

Table 2. Density ( $\rho$ ), glass transition temperature ( $T_g$ ), Young's modulus ( $E$ ), and bulk modulus ( $K$ ), Vickers hardness ( $H_v$ ), and crack resistance ( $CR$ ) of the samples in the SBN series and the SAB series

	$\rho$ (g/cm <sup>3</sup> )	$T_g$ (°C)	$E$ (GPa)	$K$ (GPa)	$H_v$ (GPa)	$CR$ (gf)
SBN1						
$x = 0.0$	2.39	483	60.0	35.7	3.7	1840
$x = 0.125$	2.45	522	68.5	43.2	4.5	270
$x = 0.25$	2.49	553	77.0	44.8	4.9	70
$x = 0.5$	2.52	571	82.0	50.6	5.4	30
$x = 0.75$	2.49	554	79.4	47.3	5.1	40
$x = 1.0$	2.44	527	74.6	46.1	4.9	70
SBN2						
$y = 0.0$	2.39	483	60.0	35.7	3.7	1840
$y = 0.5$	2.42	549	72.3	41.9	4.2	940
$y = 1.0$	2.40	598	77.0	43.1	5.1	360
SAB system						
$z = 0.0$	2.49	709	71.4	46.6	5.6	1150
$z = 2.5$	2.49	692	69.7	46.1	5.6	1420
$z = 5.0$	2.48	676	68.4	46.0	5.5	2030

Experimental uncertainties are as follows.  $d$ :  $\pm 0.01$  g/cm<sup>3</sup>,  $T_g$ :  $\pm 2^\circ$ C,  $E$ :  $\pm 1$  GPa,  $K$ :  $\pm 1$  GPa,  $H_v$ :  $\pm 0.3$  GPa.

these figures, the load at which the percentage would be 50% is determined as crack resistance or  $CR$ . The results of  $CR$  are also shown in Table 2. Relationships between  $CR$  and each compositional parameter ( $x$ ,  $y$ , and  $z$ ) are shown in Fig. 5. Results of  $\rho$  are also plotted in this figure for comparison. In the SBN1 series,  $CR$  decreases with increasing  $x$ , until  $x = 0.5$ . On the other hand,  $CR$  increases with increasing  $x$  in the region of  $x > 0.5$ . Therefore,  $CR$  shows a minimum at  $x = 0.5$ . Note that the trend of  $CR$  is opposite to that of  $\rho$ . According to Sehgal et al.,<sup>12)</sup> “brittleness” index, or susceptibility of cracking, has strong relationship with density. Brittleness of normal glass with density of more than 2.4 g/cm<sup>3</sup> increases with density. The trend agrees with that of the SBN1 series because higher  $CR$  corresponds to low brittleness index. On the other hand, there is little change in density in both the SBN2 series and the SAB series. However, the trend of  $CR$  with increase of B<sub>2</sub>O<sub>3</sub> content is different between these two series. The value of  $CR$  decreases with increasing  $y$  in the SBN2 series while  $CR$  increases with increasing  $z$ .

The diagonal length of Vickers indentation,  $2a$ , the depth of Knoop indenter before and after the heat-treatment,  $d_{\text{before}}$  and  $d_{\text{after}}$ , and  $RID$  are shown in Table 3. In the SBN1 series,  $RID$  decreases with increasing  $x$  until  $x = 0.5$ , shows a minimum at  $x = 0.5$ , and then increased. This trend is similar to that of  $CR$ , and opposite to that of  $\rho$ . In the SBN2 or the SAB series,  $RID$  does not change much with increasing  $y$  or  $z$ , respectively, although we found the changes in  $CR$  in both series.

Examples of NMR spectra in the SBN1, the SBN2, and the SAB series are shown in Fig. 6. These spectra of glass containing B<sub>2</sub>O<sub>3</sub> consist of two signals. One is a sharp signal (signal A in the figure) and the other is the broad doublet signal (signal B ~ B'). The former is originated from the four-coordinated boron, [<sup>4</sup>B], and the latter from the three-coordinated boron, [<sup>3</sup>B]. Large amount of boron is found as [<sup>4</sup>B] in the SBN1 and SBN2 series while large amount of boron is found as [<sup>3</sup>B] in the SAB series. The ratio of the amount of [<sup>4</sup>B] or [<sup>3</sup>B] to the total amount of B,  $N_4$  or  $N_3$ , respectively, is measured by deconvoluting the spectra and integrating each area. The values of  $N_4$  and  $N_3$

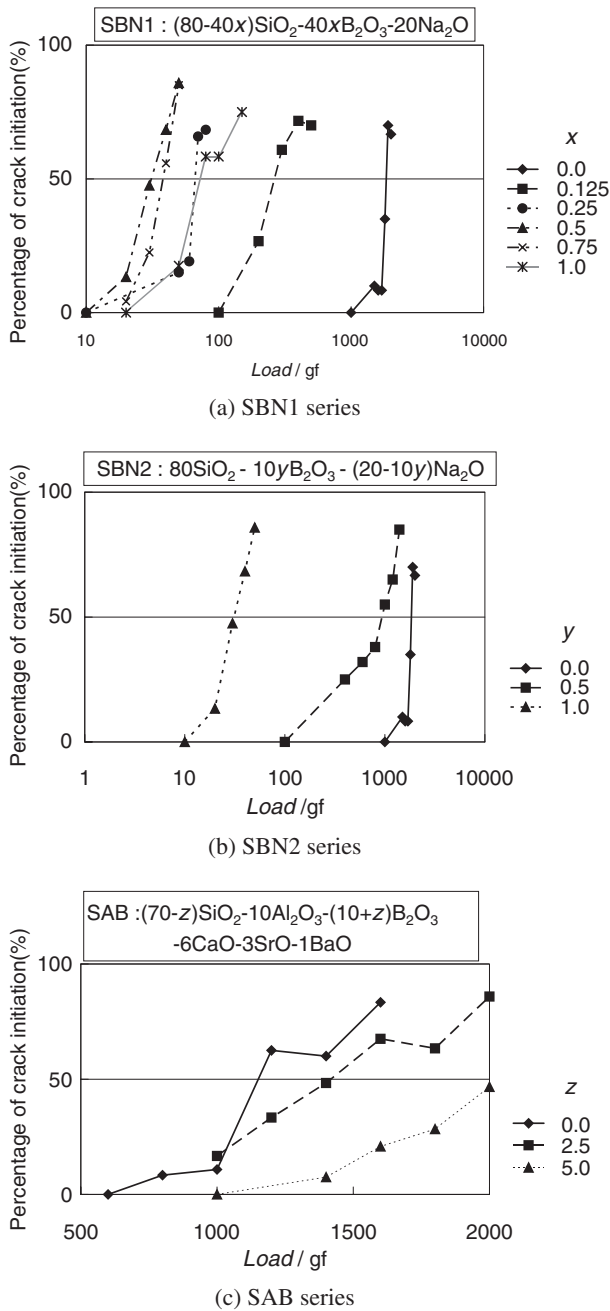


Fig. 4. A relationship between the applied load and the percentage of crack initiation. (a) SBN1 series, (b) SBN2 series, and (c) SAB series.

are shown in Table 4. Dell et al.<sup>13)</sup> showed that the ratio of  $^{[4]}\text{B}$  can be predicted from the combination of simple structural groups. For  $r\text{Na}_2\text{O}-\text{B}_2\text{O}_3-k\text{SiO}_2$  glasses ( $k \leq 8$ ),  $N_4$  is  $r$ , when  $r \leq 1/2 + K/16$ , and  $N_4$  is  $1/2 + K/16$ , when  $1/2 + K/16 \leq r \leq 1/2 + K/4$ . The results calculated by this equation are also shown in Table 4. The results in this study agree well with calculated values. The amount of the  $^{[4]}\text{B}$  unit or the  $^{[3]}\text{B}$  unit is determined as the molar content of  $\text{B}_2\text{O}_3$  multiplied by  $N_4$  or  $N_3$ , and denoted as B[4] or B[3], respectively. The amounts of B[3] and B[4] are also shown in Table 4, and plotted against each compositional parameter in Fig. 7. In the SBN1 series, B[4] increases with increasing  $x$  until  $x < 0.5$ , while B[3] does not increase. On the other hand, in the region of  $x > 0.5$ , B[3] increases with increasing  $x$  more than B[4]. It is well known that

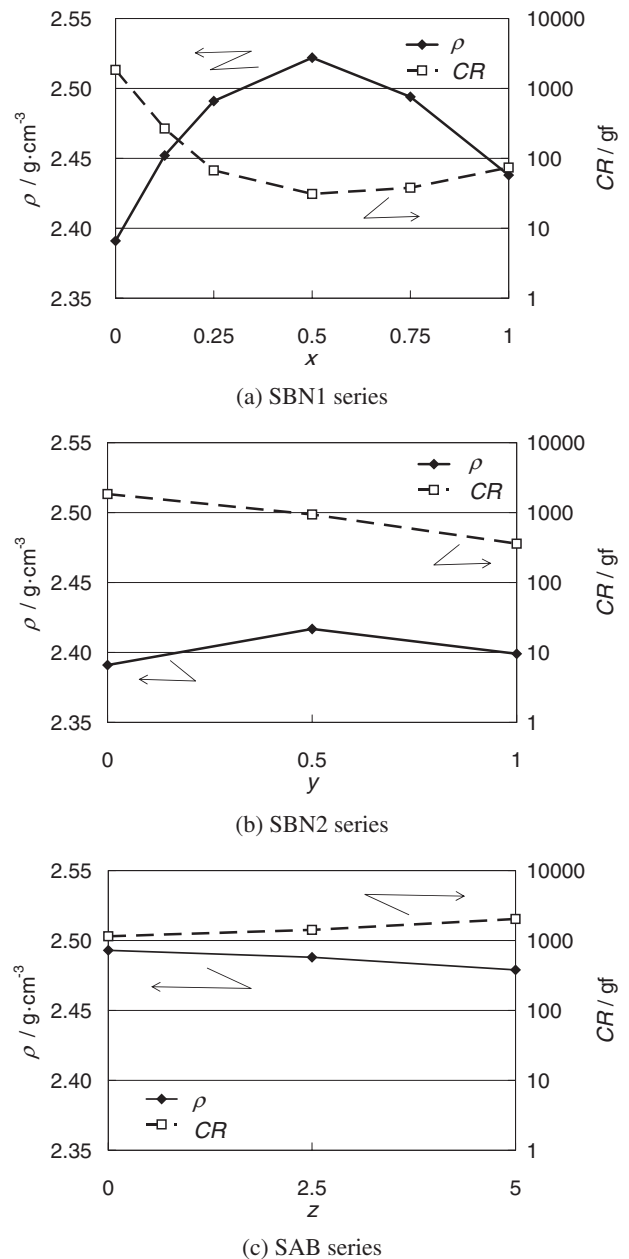
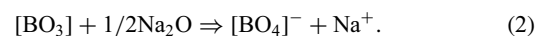


Fig. 5. Change of density and crack resistance as a function of glass compositional parameter ( $x$ ,  $y$ , and  $z$ ). (a) SBN1 series, (b) SBN2 series, and (c) SAB series.

the coordination state of boron changes by an addition of alkaline oxide as below:



Here,  $[\text{BO}_3]$  and  $[\text{BO}_4]^-$  indicate the  $^{[3]}\text{B}$  triangle unit and the  $^{[4]}\text{B}$  tetrahedral unit, respectively. Since the molar amount of  $\text{Na}_2\text{O}$  is more than that of  $\text{B}_2\text{O}_3$  in the region of  $x$  from 0.0 to 0.5, the added amount of  $\text{B}_2\text{O}_3$  changes to  $^{[4]}\text{B}$  unit. At the composition of  $x = 0.5$  (that is,  $60\text{SiO}_2-20\text{B}_2\text{O}_3-20\text{Na}_2\text{O}$ ), the amount of  $\text{B}_2\text{O}_3$  equals to that of  $\text{Na}_2\text{O}$ , so the  $^{[3]}\text{B}$  unit increases more in the range of  $x > 0.5$  because the amount of  $\text{Na}_2\text{O}$  is not enough to convert all the B[3] into B[4] through Eq. (2). Since the amount of  $\text{Na}_2\text{O}$  is much more than that of  $\text{B}_2\text{O}_3$  in the SBN2 series, the  $^{[4]}\text{B}$  unit increases with increasing the  $\text{B}_2\text{O}_3$  content.

**Table 3.** The diagonal of Vickers indentation ( $2a$ ), the depth of Knoop indentation before and after the heat-treatment at  $0.9 \times T_g$  (in °C) for 2 h, ( $d_{\text{before}}$  and  $d_{\text{after}}$ ), and recovery of indentation depth ( $RID$ ). Both of the indentations are made at the load of 100 gf

	Vickers indentation		Knoop indentation		
	$2a$ ( $\mu\text{m}$ )	$d_{\text{before}}$ ( $\mu\text{m}$ )	$d_{\text{after}}$ ( $\mu\text{m}$ )	$RID$ (%)	
<b>SBN1</b>					
$x = 0.00$	22.1	1.20	—	—	
$x = 0.125$	20.0	1.01	0.73	0.28	
$x = 0.25$	19.2	0.99	0.74	0.25	
$x = 0.5$	18.4	0.91	0.80	0.13	
$x = 0.75$	18.8	0.91	0.72	0.21	
$x = 1.00$	19.2	0.92	0.68	0.27	
<b>SBN2</b>					
$y = 0$ ( $x = 0.0$ )	22.1	1.20	—	—	
$y = 0.5$	20.7	1.02	0.697	0.32	
$y = 1.0$	18.9	0.94	0.625	0.34	
<b>SAB system</b>					
$z = 0.0$	18.0	0.99	0.61	0.39	
$z = 2.5$	18.0	1.03	0.59	0.42	
$z = 5.0$	18.3	0.98	0.56	0.42	

Experimental uncertainties are as follows.  $2a$ :  $\pm 0.3 \mu\text{m}$ ,  $d_{\text{before}}$  or  $d_{\text{after}}$ :  $\pm 0.03 \mu\text{m}$ ,  $RID$ :  $\pm 3\%$ .

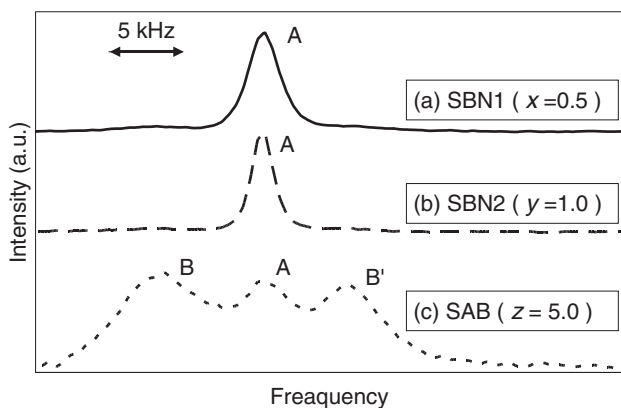
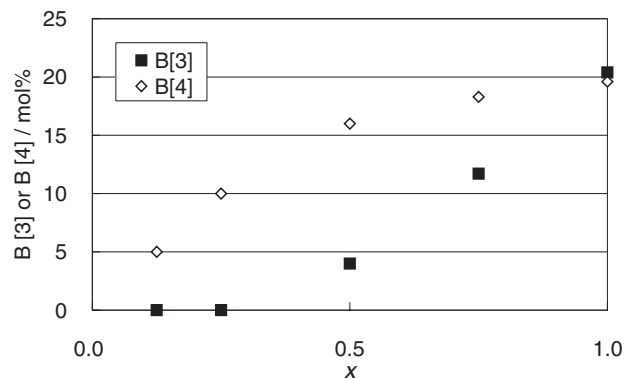


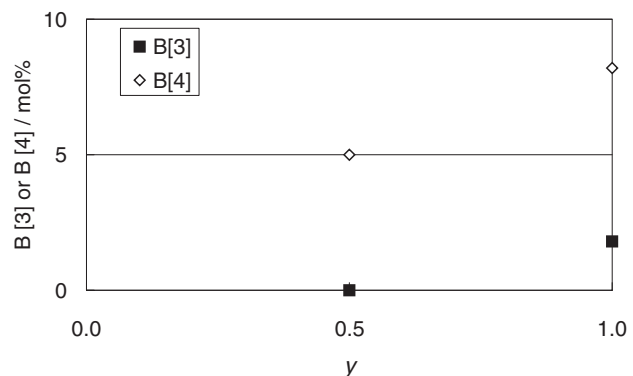
**Fig. 6.** Examples of NMR spectra in the SBN1 series, the SBN2 series, and the SAB series. (a) SBN1 series ( $x = 0.5$ ), (b) the SBN2 series ( $y = 1.0$ ), and (c) the SAB series ( $z = 5.0$ ).

**Table 4.** The ratio of 4-coordinated boron and 3-coordinated boron,  $N_4$  and  $N_3$ , and the amount of the <sup>4</sup>B unit or the <sup>3</sup>B unit. The values of the column “ $N_4$  (Dell)” are calculated according to the estimation by Dell et al.<sup>12)</sup>

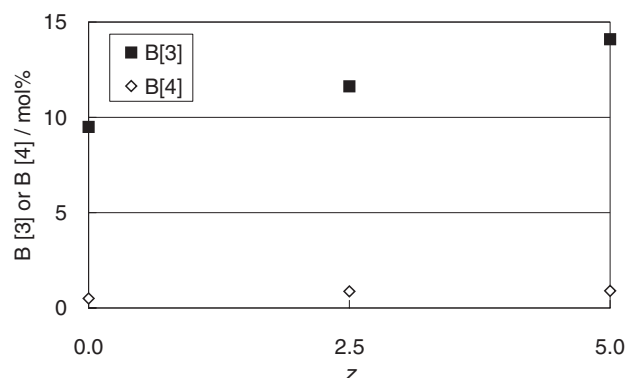
	B <sub>2</sub> O <sub>3</sub> (mol %)	$N_4$	$N_3$	B[4] (mol %)	B[3] (mol %)	$N_4$ (Dell)
$x = 0.125$	5	1.00	0.00	5.0	0.0	
$x = 0.25$	10	1.00	0.00	10.0	0.0	0.94
$x = 0.5$	20	0.80	0.20	16.0	4.0	0.69
$x = 0.75$	30	0.61	0.39	18.3	11.7	0.60
$x = 1.00$	40	0.49	0.51	19.6	20.4	0.50
<b>SBN2 series</b>						
$y = 0.5$	5	1.00	0.00	5.0	0.0	—
$y = 1.0$	10	0.82	0.18	8.2	1.8	—
<b>SAB series</b>						
SAB 0.0	10	0.05	0.93	0.5	9.5	—
SAB 2.5	12.5	0.07	0.93	0.9	11.6	—
SAB 5.0	15.0	0.06	0.94	0.9	14.1	—



(a) the SBN1 series



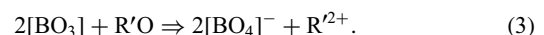
(b) the SBN2 series



(c) the SAB series

**Fig. 7.** A relationship between each compositional parameter and the amount of B[3] or B[4]. (a) the SBN1 series, (b) SBN2 series, and (c) the SAB series. B[3] and B[4] denote the molar fractions of <sup>3</sup>B unit and <sup>4</sup>B unit, respectively.

In the SAB series, which contains no alkaline ion, B[3] increased with increasing B<sub>2</sub>O<sub>3</sub>. The <sup>3</sup>B<sup>-</sup>→<sup>4</sup>B conversion reaction would also occur in non-alkaline glass due to the reaction with alkaline-earth ion (R<sup>2+</sup>) according to the following equation,



Yamashita et al. showed that alkaline-earth atom reacts more preferably with Al<sub>2</sub>O<sub>3</sub>, not with B<sub>2</sub>O<sub>3</sub> in non-alkaline aluminoborosilicate glass.<sup>14)</sup> In the SAB series, the amount of Al<sub>2</sub>O<sub>3</sub> is 15% and the total amount of R'O is about 10%, so it is estimated that all of R'O reacts with Al<sub>2</sub>O<sub>3</sub>. Therefore, the reaction shown in Eq. (3) does not occur and then B[3] increases with increasing B<sub>2</sub>O<sub>3</sub>.

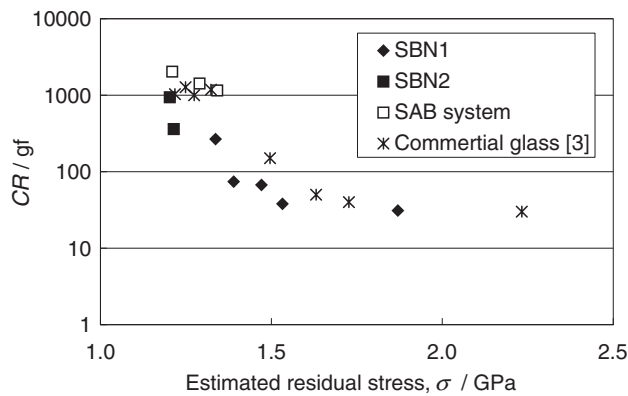


Fig. 8. A relationship between  $CR$  and the estimated residual stress,  $\sigma$ , around the indentation at a load of 100 gf. The results of commercial glasses are the results in the previous study.<sup>4)</sup>

As mentioned above,  $CR$  has strong relationship with density. In the case of the glass series without density change, effect of  $B_2O_3$  on  $CR$  depends on the glass series. Comparing Fig. 5 with Fig. 7, it is supposed that  $CR$  increases with increasing B[3] or with decreasing B[4].

#### 4. Discussion

In the previous study, we found that  $CR$  has a clear relationship with densification, or  $RID$ .<sup>4)</sup> This should be due to the fact that densification decreases the residual stress beneath the indentation,<sup>15)</sup> resulting in the increase in crack resistance. The residual stress can be derived from a simple cavity model.<sup>16)</sup> According to this model, the residual stress,  $\sigma$ , can be expressed as follows;

$$\sigma = K \cdot \Delta V / V. \quad (4)$$

Here,  $\sigma$  is the estimated residual stress,  $K$  is the bulk modulus, and  $\Delta V$  the indentation volume and  $V$  the volume of plastic zone around the indentation. By modifying Eq. (4), the residual stresses around the indentation of various commercial glasses were estimated in the previous study.<sup>4)</sup> In the previous study, the followings are assumed for the modification; (1) the diameter of hemispherical plastic zone is equal to that of the Vickers indentation diagonal,  $2a$ ,<sup>17)</sup> (2)  $\Delta V$  equals to the volume of the indentation after the heat-treatment, and (3)  $d_{\text{after}}$ , which is depth of Knoop indentation after the heat-treatment at the  $RID$  measurement, is proportional to the value of  $d_{\text{after}}^V$ , which is depth of Vickers indentation after the heat-treatment for all of the glass compositions ( $d_{\text{after}}^V = 1.34 \cdot d_{\text{after}}$ ). Finally, the residual stress around the indentation was estimated to be as follows:

$$\sigma = 0.427 \cdot K \cdot d_{\text{after}} / a. \quad (5)$$

Details of the assumption were described in our previous paper.<sup>4)</sup> The calculated residual stress is shown in Fig. 8. The results of the commercial glass in the previous study<sup>4)</sup> are also shown in this figure for comparison. The value of  $CR$  decreases with increasing the residual stress in the SBN series and the SAB series, similar to the results of commercial glasses.

As shown in Eq. (5), the residual stress is affected by bulk modulus and the value of  $d_{\text{after}}/a$ . The value of  $d_{\text{after}}/a$  correlates with the ratio of the cavity radius to the radius of plastic zone. The smaller value of  $1/a$ , or the smaller hardness, indicates the more plastic deformation, while the smaller  $d_{\text{after}}$  indicates larger annealing recovery, or less shear flow. Therefore, the value of  $d_{\text{after}}/a$  is one measure of contribution of densification. The larger contribution of densification corresponds to the smaller value of

Table 5. Regression coefficient,  $\beta(NWF)$ , of logarithm of  $CR$  with four variable, e.g., the molar fraction of  $^{[3]}B_2O_3$ ,  $^{[4]}B_2O_3$ ,  $SiO_2$ , and  $Al_2O_3$ , and intercept,  $C$ , obtained by multivariable linear regression analysis

Regression coefficient, $\beta(NWF)$	
$^{[3]}B_2O_3$	+0.098
$^{[4]}B_2O_3$	-0.092
$SiO_2$	+0.038
$Al_2O_3$	-0.067
Intercept, $C$	
	+0.179

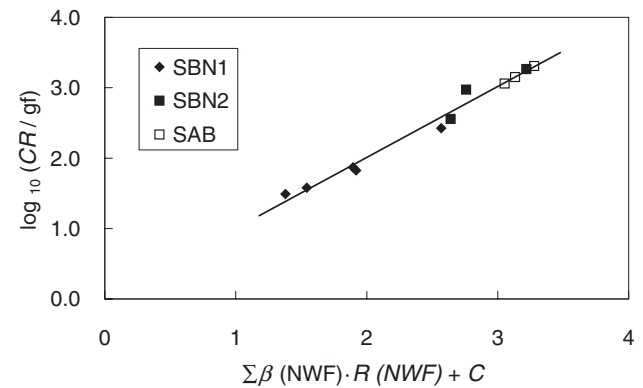


Fig. 9. Comparison between the value of  $\log_{10} CR$  and the value of  $\Sigma \beta(NWF) \cdot R(NWF) + C$ . Here,  $\beta(NWF)$  and  $R(NWF)$  are regression coefficient and molar fraction of network component  $NWF$ , respectively, and  $C$  is an intercept. The regression coefficients of  $\beta(NWF)$  are obtained by multivariable linear analysis.

$d_{\text{after}}/a$ , resulting in the smaller residual stress which would be driving force of crack initiation. The  $RID$  values measured in this study were also another measure of densification, which is proportional to the value of  $d_{\text{after}}/a$ .

As mentioned above, it seems that effect of  $B_2O_3$  on  $CR$  depends on the coordination state of boron. However, since network structure should affect  $CR$ , effects of  $SiO_2$  and  $Al_2O_3$  also have to be taken into account. Then, by multivariable linear regression analysis for logarithm of  $CR$ , regression coefficients of molar fraction of  $^{[3]}B_2O_3$ ,  $^{[4]}B_2O_3$ ,  $SiO_2$ , and  $Al_2O_3$  were obtained, which indicate effect of each component on  $\log_{10} CR$ . That is, the value of  $\log_{10} CR$  is approximated as the following equation;

$$\log_{10} CR = \Sigma \beta(NWF) \cdot R(NWF) + C, \quad (6)$$

where  $\beta(NWF)$  and  $R(NWF)$  are regression coefficient and molar fraction of the network component  $NWF$ , respectively, and  $C$  is an intercept. The regression coefficients and the intercept are listed in Table 5. The value of  $\log_{10} CR$  is plotted against the value of  $\Sigma \beta(NWF) \cdot R(NWF) + C$ , in Fig. 9. The correlation coefficient for the analysis of 0.99 is obtained. The effects of  $^{[3]}B_2O_3$  and  $SiO_2$  are positive while the effects of  $^{[4]}B_2O_3$  and  $Al_2O_3$  are negative. It indicates that  $^{[3]}B_2O_3$  and  $SiO_2$  increase  $CR$  and that  $^{[4]}B_2O_3$  and  $Al_2O_3$  decrease.

It is considered that the large effect of  $^{[3]}B_2O_3$  is due to the following three factors: single bond strength, openness, and planar structure. Since crack initiation corresponds to break of network bond, it is reasonable that high single bond strength increase  $CR$ . The order of single bond strength with oxygen:<sup>18)</sup>  $^{[3]}B-O$  (499 kJ/mol) >  $Si-O$  (444 kJ/mol) >  $Al-O$  (293-423 kJ/mol) >  $^{[4]}B-O$  (373 kJ/mol) agree with that of the effect on  $\log_{10} CR$ . However, the single bond strength is not much different among them. Therefore, the openness and the planar

structure of <sup>[3]</sup>B<sub>2</sub>O<sub>3</sub> unit have more effects on *CR* than the bond strength. The open structure leads to an easy densification by indentation, resulting in a small residual stress. The tetrahedra of <sup>[4]</sup>BO<sub>4</sub> and AlO<sub>4</sub> are accompanied with modifier cations in the glass network for charge compensation, to make the network more packed. On the other hand, the SiO<sub>4</sub> tetrahedron and the <sup>[3]</sup>BO<sub>3</sub> planar triangle do not need such charge compensation, so they make open network structure. The specific planar structure of <sup>[3]</sup>B unit would also contribute to a large densification. The introduction of the <sup>[3]</sup>B planar triangle unit into main SiO<sub>2</sub> network makes the network less rigid, which allows densification under a stress. It is deduced that the open network and the planar structure cause an easier densification. For further discussion, it will be needed to get an insight into the intermediate range order of <sup>[3]</sup>B<sub>2</sub>O<sub>3</sub> containing glass under a stress.

### 5. Conclusion

By using glasses in the SiO<sub>2</sub>-B<sub>2</sub>O<sub>3</sub>-Na<sub>2</sub>O ternary (SBN) series and non alkaline aluminoborosilicate (SAB) series, effect of B<sub>2</sub>O<sub>3</sub> content on crack resistance (*CR*) was investigated. The value of *CR* has a relationship with density in the SBN system. In the SBN2 series where density does not change with B<sub>2</sub>O<sub>3</sub> content, *CR* decreases with increasing B<sub>2</sub>O<sub>3</sub>. On the other hand, *CR* increases with increasing B<sub>2</sub>O<sub>3</sub> content in the SAB series where density does not change, neither. From the results of NMR spectra, it is found that the reason of the difference is due to the difference in the coordination state of boron. The value of *CR* increases with increasing 3-coordinated boron <sup>[3]</sup>B and decreasing 4-coordinated boron <sup>[4]</sup>B. The value of *CR* has a relationship with the residual stress around the indentation. The open network and the planar structure of <sup>[3]</sup>B unit should result in an increase in contribution of the densification and a decrease in the residual stress.

### References

- 1) M. Wada, H. Furukawa and K. Fujita, *Proc. of X International Congress on Glass*, **11**, 39–169 (1974).
- 2) B. R. Lawn and D. B. Marshall, *J. Am. Ceram. Soc.*, **62**, 347–350 (1979).
- 3) J. Sehgal, Y. Nakao, H. Takahashi and S. Ito, *J. Mater. Sci. Lett.*, **14**, 167–169 (1995).
- 4) Y. Kato, H. Yamazaki, S. Yoshida and J. Matsuoka, *J. Non-Cryst. Solids*, under refereed.
- 5) I. Ohno, *J. Phys. Earth*, **24**, 355–379 (1976).
- 6) J. E. Neely and J. D. Mackenzie, *J. Mater. Sci.*, **3**, 603–609 (1968).
- 7) S. Yoshida, S. Isono, J. Matsuoka and N. Soga, *J. Am. Ceram. Soc.*, **84**, 2141–2143 (2001).
- 8) S. Yoshida, J.-C. Sanglebouef and T. Rouxel, *J. Mater. Res.*, **20**, 3404–3412 (2005).
- 9) S. Yoshida, J.-C. Sanglebouef and T. Rouxel, *Int. J. Mater. Res.*, **98**, 360–364 (2007).
- 10) J. D. Mackenzie, *J. Am. Ceram. Soc.*, **46**, 470–476 (1963).
- 11) H. Miyoshi, D. Chen, H. Masui, T. Yazawa and T. Akai, *J. Non-Cryst. Solids*, **345–346**, 99–103 (2004).
- 12) J. Sehgal and S. Ito, *J. Non-Cryst. Solids*, **253**, 126–132 (1999).
- 13) W. J. Dell, P. J. Bray and S. Z. Xiao, *J. Non-Cryst. Solids*, **58**, 1–12 (1983).
- 14) H. Yamashita, K. Inoue, T. Nakajin, H. Inoue and T. Maekawa, *J. Non-Cryst. Solids*, **331**, 128–136 (2003).
- 15) R. F. Cook and G. M. Pharr, *J. Am. Ceram. Soc.*, **73**, 787–817 (1990).
- 16) B. R. Lawn, A. G. Evans and D. B. Marshall, *J. Am. Ceram. Soc.*, **63**, 574–581 (1980).
- 17) E. H. Yoffe, *Philos. Mag. A*, **46**, 617–628 (1982).
- 18) K. H. Sun, *J. Am. Ceram. Soc.*, **30**, 277–281 (1947).